

Multielectron dissociative ionization of diatomic molecules in an intense femtosecond laser field

C. Cornaggia, J. Lavancier, D. Normand, J. Morellec, and P. Agostini
*Service de Physique des Atomes et des Molécules, Centre d'Etudes de Saclay,
 91191 Gif-sur-Yvette CEDEX, France*

J. P. Chambaret and A. Antonetti
*Laboratoire d'Optique Appliquée, Ecole Nationale Supérieure de Techniques Avancées,
 Ecole Polytechnique, 91120 Palaiseau, France*

(Received 30 April 1991)

The multielectron dissociative ionization of diatomic molecules is investigated using an intense laser field at a wavelength of 615 nm, in the 10^{15} W/cm² intensity range, with a 100-fs pulse duration. Comparison with previous experiments performed with 2-ps and 600-fs pulse durations shows that the atomic-ion kinetic-energy releases depend neither on the laser-pulse duration nor on the peak laser intensity. The simple model of Coulomb repulsion between atomic ions is therefore insufficient to account for the dynamics of the multiple-ionization mechanism. Comparison between N₂, CO, and O₂ experiments indicates that the channel $AB^{2+} \rightarrow A^+ + B^+$ remains molecule specific. Conversely, the channels involving molecular ions carrying higher charges ($AB^{(p+q)+} \rightarrow A^{p+} + B^{q+}$) exhibit similar dissociation energies for N₂, CO, and O₂.

PACS number(s): 33.80.Rv, 33.80.Eh

I. INTRODUCTION

The molecular response to an intense radiation field is a subject of growing interest. For diatomic molecules, the multielectronic dissociative ionization has recently attracted a lot of attention [1–14]: the interaction can lead to the formation of transient multicharged molecular ions that dissociate into energetic fragments. The measurement and analysis of the fragment kinetic energies provide a powerful method to investigate the excitation pathways of the molecules [1]. In principle, the multiphoton-ionization steps can occur along the so-called “vertical” or “nonvertical” paths. For the first one, the ionization sequence occurs at the equilibrium internuclear distance of the neutral molecule, as established for N₂ at 248 nm [3] and 305 nm [4] and for CO at 305 nm [10]. For the second one, the sequence progresses at increasing internuclear distances, that is during the dissociation of the transient molecular ion, as found for N₂ (Refs. [1], [2], and [4]), HI (Ref. [5]), CO (Refs. [7]–[10]) around 600 nm and for O₂ at 305 and 610 nm [11]. The vertical or nonvertical character of the molecular excitation was interpreted to be governed by the lifetime τ of the doubly charged states [12]. When τ is much larger than the pulse duration, the process is vertical. On the contrary, when the time scale of the dissociation is much shorter than the pulse duration, the multiple-ionization process is nonvertical.

Previous experiments have established that the fragment energies are, to a large extent, independent of the laser intensity, in the range of 10^{13} – 5×10^{15} W/cm². In a classical Coulomb repulsion model, this implies that the multiphoton ionization of the dissociating molecular ions occurs at fixed internuclear distances whatever the peak laser intensity [4,10,11]. A possible interpretation can be

based on the fact that a particular ionization such as



(where L represents a laser) appears when the necessary threshold laser intensity is available in the laser-pulse duration envelope. In this picture, the atomic ions, arising from the dissociation of the molecular ion [AB^{q+}], separate during the pulse rise time until this threshold value is reached. Then, the internuclear distances at which the successive ionizations occur depend on the time duration necessary to connect the threshold laser intensities. Therefore, in this simple interpretation, the temporal dynamics of the dissociation is expected to be governed by the rise time of the laser pulse. The experiments, so far, have been limited to picosecond or slightly subpicosecond pulses. The recent development of lasers delivering ultrashort (100 fs) intense (10^{16} W/cm²) pulses has significantly enlarged the fields of investigation. The aim of this work was to explore the dynamics of the nonvertical process for very short pulse duration.

In order to test the predictions of the simple Coulomb repulsion model, we have performed a series of experiments with a 100-fs pulse duration laser at 615 nm with intensities up to 3×10^{15} W/cm². This pulse duration corresponds to the classical time scale for Coulomb repulsion which is in the range of several tens of femtoseconds for internuclear motion over a few angstroms. In this case, both the excitation source rise time and the target “classical” response have similar time scales. The diatomic molecules under investigation are N₂, CO, and O₂ for which there are comparable measurements at 600 and 610 nm but with different laser-pulse durations, respectively, 600 fs [1,2,7–9] and 2 ps [4,10,11].

The paper is organized as follows. Section II gives a brief description of the experimental apparatus. Section

III describes the identification methods of the fragmentation channels and presents the experimental findings. The discussion of the experimental results is organized in three subsections. In Sec. IV A, we investigate in detail the excitation pattern of N_2 and we compare the ion kinetic-energy releases obtained in the present experiment with previous measurements performed at the same intensity level but with longer pulse duration. In Sec. IV B, we discuss the laser intensity effects on the energy of the fragments and on the branching ratios to different dissociative channels. Finally, in Sec. IV C we compare the molecular responses of N_2 , CO, and O_2 .

II. EXPERIMENTAL SETUP

The laser is an upgraded version of the standard system described elsewhere [15]. Briefly, the 0.1-nJ, 50-fs laser pulses delivered by a colliding-pulse mode-locker oscillator are amplified up to 2 mJ in a five-stage dye amplifier (Bethune cells) pumped by a single-mode Nd-YAG (where YAG represents yttrium aluminum garnet) laser operating at 20 Hz. Due to group velocity dispersion in the amplifiers, the pulses are broadened to 150 fs and subsequently recompressed by a double pass two-prism device to 80 fs [full width at half maximum (FWHM)]. With a 70-mm achromat lens, this beam can be focused to $10 \mu\text{m}^2$ resulting in peak intensities in excess of 10^{17} W/cm^2 . In the present experiment, using a 150-mm lens, the beam can be focused down to a spot of $200 \mu\text{m}^2$. Owing to the difference between the phase and group velocities, the pulse front is delayed with respect to the phase front [16] resulting in an effective pulse duration of 100 fs. These characteristics lead to peak intensities of $3 \times 10^{15} \text{ W/cm}^2$.

The experimental setup to measure the kinetic energies of the atomic ions is the same that we used previously in the picosecond experiments [4]. The detection system consists of a double chamber time-of-flight (TOF) ion mass spectrometer pumped at a background pressure of 10^{-9} Torr [17]. The application of a weak extraction electric field in the interaction chamber makes it possible to determine the fragment kinetic energies with a good accuracy (10%) whereas the second chamber strongly accelerates the ions to ensure a good collection efficiency. Finally, the ions are mass separated through an 18-cm-long drift tube and give a signal which feeds a Lecroy model 9400 Transient Digitizer with a 100-MHz sampling frequency.

III. EXPERIMENTAL RESULTS

A typical TOF spectrum obtained from the multielectronic dissociative ionization of N_2 is presented in Fig. 1 (wavelength 615 nm; pulse duration 100 fs; laser intensity $2.5 \times 10^{15} \text{ W/cm}^2$). The TOF spectrum is dominated by the N_2^+ molecular-ion species with a comparatively low N_2^{2+} molecular-ion signal. In the 10^{15} W/cm^2 range, we have verified that the N_2^+ ion yield is saturated as a function of the laser intensity. This saturation means that in the central part of the laser spot the molecules are excited to higher charged states via the N_2^+ states, whereas the

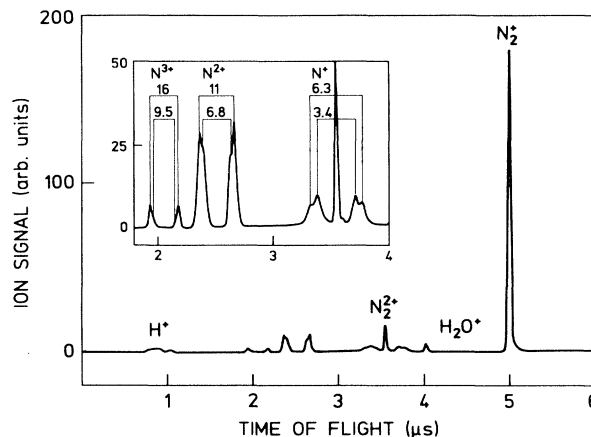


FIG. 1. TOF ion mass spectrum of N_2 recorded with 100-fs pulse duration, 615-nm wavelength, and $2.5 \times 10^{15} \text{ W/cm}^2$ laser intensity. The extraction field in the interaction chamber is 60 V/cm and the N_2 pressure is 3.5×10^{-8} Torr. The top left window shows the N^+ , N_2^{2+} , N^{2+} , N^{3+} TOF ion mass spectrum recorded with N_2 pressure of 1.2×10^{-7} Torr.

detected N_2^+ ions come from the outer part of the spot where the laser intensity is lower. Each atomic-ion species is characterized by a double peak structure, when the laser polarization lies along the detection axis. The faster component represents ions initially ejected toward the detector (“toward component”) while the slower component comes from ions initially released in the opposite direction and whose momenta have been reversed by the extraction electric field (“away component”). The ion kinetic energies are determined from the difference of time of flight between the “away” and “toward” components. In order to improve the statistics of our measurements, the kinetic energies are measured for several extraction fields ranging from 30 to 70 V/cm, and then averaged over the whole set of data. The error bar is found to be $\pm 10\%$ of the final result. The atomic-ion kinetic-energy releases are summarized in Tables I, II, and III for, respectively, N_2 , CO, and O_2 and compared with previous results obtained at 2 ps [4,10,11] and 600 fs [1,2,7–9]. The last two columns of each table correspond to the dissociative channels associated with the measured kinetic energies. A particular channel can appear two times in the tables if it is composed of two different atomic fragments.

The identification of each channel composed of two repelling atomic ions is based on (i) the conservation of momentum and energy of the parent molecular ion, (ii) the same abundance of the associated atomic ions, and (iii) the same laser intensity dependence for both ions. Concerning criterion (ii), the relative abundances of different charge state ions have to be corrected for the gain of the electron multiplier. The secondary emission factors of a CuBe dynode have been measured for impinging noble gas ions with accelerating voltages ranging from 3 to 10 kV [18]. According to these data, the elec-

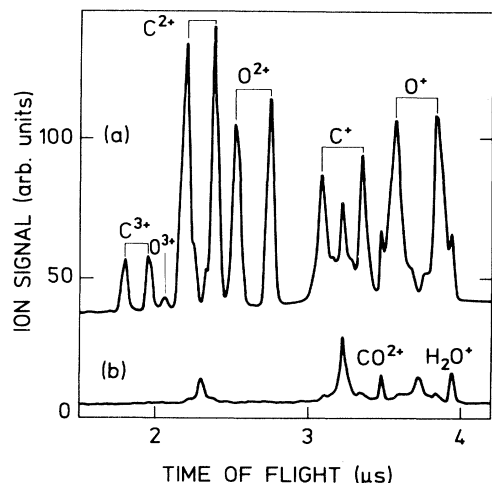


FIG. 2. TOF ion mass spectra of CO with the laser polarization (a) parallel to the drift tube axis and (b) perpendicular to the drift tube axis. The scale for the ion signals is the same for both spectra.

tron multiplier gain is found to be almost proportional to $Z/M^{1/2}$ where Z and M represent, respectively, the charge state and the mass of the impinging ion. Our results based on criteria (i), (ii), and (iii) are found to be in good agreement with those obtained by Frasiniski and co-workers using covariance mapping techniques [2,8].

The angular distribution of atomic ions relative to the laser polarization is found to be strongly peaked along the E vector of the laser field. As an illustration, we show in Fig. 2 the TOF ion mass spectra of CO recorded for two orthogonal polarizations of the laser field. In Fig. 2(a), the E field is parallel to the drift tube axis (this is the usual situation for measuring the ion energies). In Fig. 2(b), the laser polarization is set at a right angle: the fragments are then ejected to 90° from the detection axis and cannot enter the second acceleration chamber through the 10-mm aperture of our TOF spectrometer.

Thereby, the energetic ion fragments are lost; we only detect the low-energy atomic ions C^+ and thermal molecular ions (CO^{2+} and parasitic H_2O^+ ions). The observed angular distributions are in agreement with previous experiments performed with 600-fs and 2-ps laser-pulse duration [9,10]. In the field ionization model [2], a diatomic molecule is more easily ionized when its axis lies along the laser E field because of its elongated shape. For (sub)picosecond laser pulses, there is no time for molecular rotation during the pulse duration and the resulting atomic ions are ejected along the laser electric field.

IV. DISCUSSION

A. Fragmentation channels observed at 100 fs: Comparison with 2-ps and 600-fs experiments

The fragmentation channels observed at 100 fs are essentially the same as those deduced from our previous experiments at 2 ps [4,10,11]. However, we made some reassignments in the fragmentation channels involving triple charged ions. Indeed, the assignment of these channels is difficult because atomic A^{3+} ion signals are weak and because of the different electron multiplier responses to different ion charge states. For instance, the channel $AB^{4+} \rightarrow A^{3+} + B^+$ will yield a weak A^{3+} signal and a 3 times smaller B^+ signal which will surimpose to the strong B^+ signal coming from $AB^{2+} \rightarrow A^+ + B^+$.

For instance, the 9.5-eV N^{3+} signal (Fig. 1) was previously assumed to arise from the subsequent ionization of atomic N^{2+} ions. With 100-fs pulses, the subsequent ionization of fragments becomes very unlikely. Therefore we assume that the 9.5-eV N^{3+} are issued from the channel $N^{4+} \rightarrow N^{3+} + N^+$ (there is indeed some signal at 10 eV in the wings of the N^+ peak). Moreover, the 16-eV N^{3+} ions were previously identified as coming from the $N^{3+} + N^{3+}$ channel [1,4]. In fact, the covariance mapping technique established that these ions were due to $N_2^{5+} \rightarrow N^{2+} + N^{3+}$ (Ref. [2]). The N^{3+} ion assignments are summarized in Table I according to these more recent data.

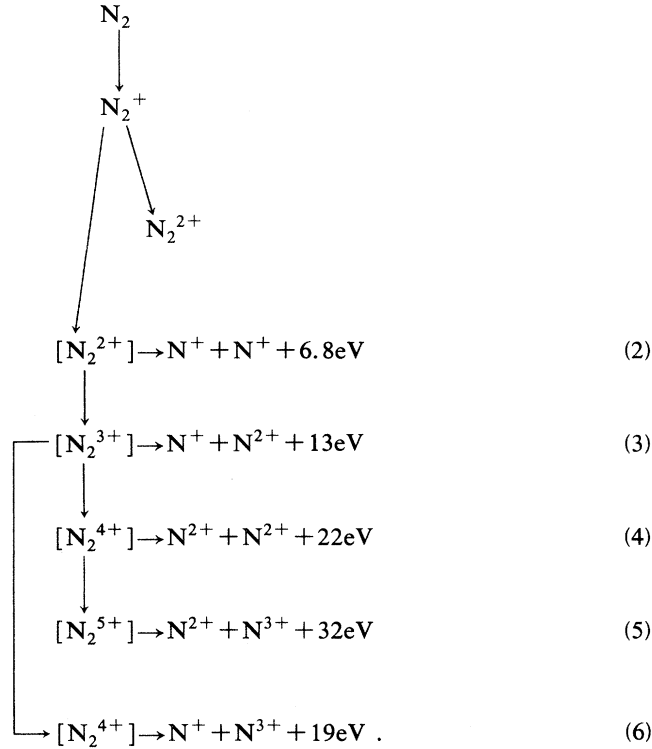
We proceed in the same way for CO and O_2 with, respectively, C^{3+}, O^{3+} and O^{3+} atomic ions. In Table II, the 10-eV C^{3+} ion is assigned to the $C^{3+} + O^+$ fragmen-

TABLE I. Measured atomic-ion kinetic energies following the multielectron dissociative ionization of N_2 for different laser-pulse durations. The last column is devoted to the identification of the dissociative channels (see text).

Atomic ion	Ion kinetic-energy release (eV)			Fragmentation channel	Channel number
	2 ps Ref. [10]	600 fs Ref. [8]	100 fs This work		
N^+	3.5	3	3.4	$N^+ + N^+$	1
	5.8	6.5	6.3	$N^+ + N^{2+}$	2
N^{2+}	6.2	6.5	6.8	$N^+ + N^{2+}$	2
	10	11	11	$N^{2+} + N^{2+}$	3
N^{3+}	9	10	9.5	$N^+ + N^{3+}$	4
	14	15	16	$N^{2+} + N^{3+}$	5

tation channel in agreement with the covariance mapping results [8]. The 17-eV C^{3+} ions and 14-eV O^{3+} ions are, respectively, assigned to $C^{3+} + O^{2+}$ and $C^{2+} + O^{3+}$ channels although we cannot resolve the corresponding double charged ion peaks. Finally, in the case of O_2 , the O^{3+} ions are assumed to arise from the dissociation of O_2^{4+} into $O^{3+} + O^+$ ions.

Our results are illustrated by the following excitation pattern for N_2 :



The conventions of the above diagram are as follows. The vertical arrows correspond to the removal of one electron whereas the horizontal arrows denote a dissociation channel without any electronic emission. The transient molecular ions are mentioned in brackets. We detect both N_2^+ and N_2^{2+} molecular ions as illustrated in Fig. 1. The N_2^{2+} signal is due to molecular dictations whose lifetimes are greater than $3.5 \mu\text{s}$. Their appearance laser intensity indicates that they are not the parent molecular ions generating the 3.4-eV N^+ ions. In reaction (2), the short-lived states of N_2^{2+} are assumed to be $A^3\Sigma_g^-$ and/or $b^1\Pi_u$ in good agreement with synchrotron experiment [19] and electron-impact experiments [20].

The measured kinetic-energy releases can be explained by the successive multiphoton ionizations of the dissociating transient ions at internuclear distances greater than the N_2^{2+} equilibrium distance. Following the classical Coulomb repulsion model, the kinetic energies are much less than those expected in a vertical excitation. Since the measured atomic-ion energy distributions are peaked around well-defined values (Fig. 1), the ionizations occur at fixed internuclear distances which can be deduced from classical mechanics. The transitions $N_2^{2+} \rightarrow N_2^{3+}$ and $N_2^{3+} \rightarrow N_2^{4+}$ occur, respectively, at 2.2 and 3.2 Å but $N_2^{4+} \rightarrow N_2^{5+}$ happens at 2.9 Å, which is smaller than 3.2 Å for the preceding step. The sequence of successive ionization steps is therefore not so straightforward as deduced from a simple classical Coulomb repulsion.

The most striking feature of this experiment is that the atomic-ion kinetic-energy releases do not depend on the laser-pulse duration. Indeed, the kinetic energy released in a given dissociative channel (cf. Tables I–III) is found to be the same with 2-ps, 600-fs, and 100-fs laser-pulse durations (within the 10% error bar). This observation proves that the molecular dynamics is, to a large extent, uncorrelated with the laser-pulse rise time as pointed out

TABLE II. Measured atomic-ion kinetic energies following the multielectron dissociative ionization of CO for different laser-pulse durations. The last column is devoted to the identification of the dissociative channels.

Atomic ion	Ion kinetic-energy release (eV)			Fragmentation channel	Channel number
	2 ps Ref. [10]	600 fs Ref. [8]	100 fs This work		
C^+	3.3	3.8	3.7	$C^+ + O^+$	1
	6.5		6.4	$C^+ + O^{2+}$	2
O^+	2.5	2.8	2.9	$C^+ + O^+$	1
	4.4		5.0	$C^{2+} + O^+$	3
C^{2+}	5.4	6.2	6.5	$C^{2+} + O^+$	3
	11	12	11	$C^{2+} + O^{2+}$	4
O^{2+}	4.8	4.8	5.3	$C^+ + O^{2+}$	2
	8.1	9.3	8.9	$C^{2+} + O^{2+}$	4
C^{3+}	7.9	10	10	$C^{3+} + O^+$	5
			17	$C^{3+} + O^{2+}$	6
O^{3+}			14	$C^{2+} + O^{3+}$	7

TABLE III. Measured atomic-ion kinetic energies following the multielectron dissociative ionization of O_2 for different laser-pulse durations. The last column is devoted to the identification of the dissociative channels.

Atomic ion	Ion kinetic-energy release (eV)		Fragmentation channel	Channel number
	2 ps Ref. [11]	100 fs This work		
O^+	2.4	2.8	$O^+ + O^+$	1
		6.3	$O^+ + O^{2+}$	2
O^{2+}	6.3	5.6	$O^+ + O^{2+}$	2
		11	10	$O^{2+} + O^{2+}$
O^{3+}	6.3	9.0	$O^+ + O^{3+}$	4
		17	16	$O^{2+} + O^{3+}$

recently by Codling, Frasinski, and Hatherly for pulse durations in the range 0.2–2 ps [21]. In our opinion, this shows the limits of the Coulomb explosion model: we make the assumption that the dissociation of the molecular ions may be slowed down by some screening effects due to the electrons. In addition, the description of the excitation pattern would require a full quantum treatment. Particularly the motion of the still correlated atomic ions during ionization and a more detailed interaction than the pure Coulomb one remains to be investigated using quantum mechanics.

B. Laser intensity effects

The laser intensity dependence of the multielectronic dissociative ionization was found to provide essential information about the dynamics of the excitation pattern and the identification of the dissociation channels following point (iii) in Sec. III [4,10,11]. The fragmentation channels reported in Tables I–III at 100 fs were partly deduced from this point in association with the criteria (i) and (ii) as we mentioned earlier. The spectra recorded at 100 fs and 615 nm for N_2 at two different laser intensities 2×10^{15} and 10^{14} W/cm² are presented in Figs. 3(a) and 3(b). At high intensity, the operating pressure was reduced by two orders of magnitude to avoid saturation of the detector.

The main feature appearing in Figs. 3(a) and 3(b) is that both spectra exhibit the same ion energies for different laser intensities. At 2×10^{15} W/cm², the $N^{2+} + N^{2+}$ channel dominates the other channels while at 10^{14} W/cm², the $N^+ + N^+$ channel is the more important. Spectra recorded at different laser intensities show that the $N^+ + N^{2+}$ channel is never the prominent one (it always gives fewer atomic ions than the symmetric channels $N^+ + N^+ + N^{2+}$). This could be explained by the asymmetric character of this channel: an electron belonging to N^+ , attracted by the higher electric field of N^{2+} can move off the N^+ atom to a region of the large internuclear gap between the ions where the binding field is lower, and thus be more easily removed.

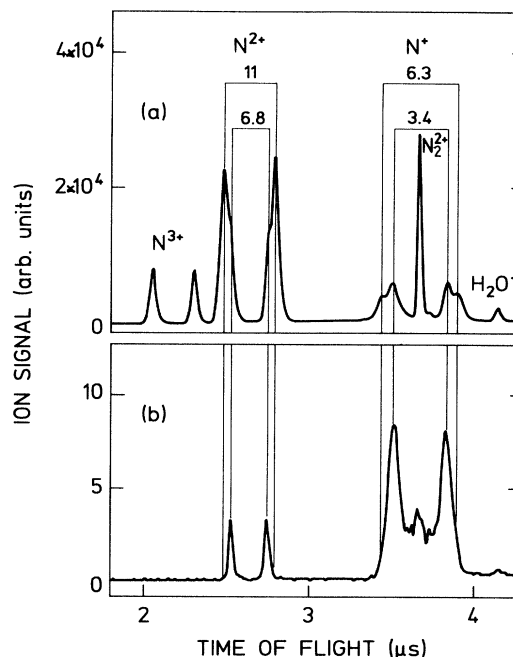


FIG. 3. TOF ion mass spectra of N_2 at 615 nm with 100-fs pulse duration for two peak intensities: (a) 2×10^{15} W/cm² and (b) 10^{14} W/cm². The N_2 operating pressure is, respectively, 3.5×10^{-7} and 5×10^{-5} Torr. The vertical axis is the pressure normalized ion signal.

The fact that the ion energies are independent of the laser-pulse peak intensity could be an indication of an intensity-tuned resonance process. In this case, since the resonance signals stand out over the nonresonant background, the experiment selects the resonant events which occur at those intensities which adjust the resonances, whatever the peak intensity is. Such a situation is met in the multiphoton ionization of atoms under strong laser field conditions [22,23]. Different resonant processes may occur during the same laser pulse at different spatiotemporal points in the interaction volume. The resulting signals are of course depending on the effective volumes where the resonance condition is satisfied. In the present case, resonances in the system of two repelling atomic ions could induce multiphoton ionization at well-determined internuclear distances and would give the same ion kinetic energies independently of the peak laser intensity. In the case of molecular systems, however, the internal structure is so rich that these ac Stark tuned resonances would be some kind of “giant resonances” which would dominate the excitation and explain the relatively low number of observed fragmentation channels.

C. Comparison of N_2 , CO, and O_2

The last investigated point is the molecular response as a function of the molecule. In Table IV, we summarize

TABLE IV. Total kinetic-energy releases in the fragmentation channels following the multielectron dissociative ionization of N_2 , CO, and O_2 in intense laser field with 100-fs pulse duration, 615-nm wavelength in the 10^{15} W/cm² range.

Fragment channel	Molecule	N_2	CO	O_2
	AB			
$A^+ + B^+$		6.8	6.6	5.5
$A^+ + B^{2+}$			11.7	
$A^{2+} + B^+$		13.1	11.7	11.9
$A^{2+} + B^{2+}$		22	19.9	20
$A^{2+} + B^{3+}$			32.7	
$A^{3+} + B^{2+}$		32	29.8	32

the total kinetic-energy releases and the associated fragmentation channels observed with 100-fs pulse laser duration for N_2 , CO, and O_2 . Since we do not observe significant changes for different laser-pulse durations and laser intensities, the following discussion can be applied to the 2-ps data [4,10,11] as well.

The general trend observed in Table IV consists in the quite similar energies measured for equivalent dissociation channels of N_2 , CO, and O_2 . A simple explanation can be based on the fact that these molecules are constituted of neighboring atoms in the periodic table of the elements. Moreover N_2 and CO are isoelectronic molecules. The O_2 molecule has the electronic structure of N_2 plus two antibonding electrons. This simple statement explains why the $N^+ + N^+$ and $C^+ + O^+$ channels exhibit almost the same dissociation energy while the $O^+ + O^+$ channel appears with a somewhat lower energy.

Concerning the fragmentation channels other than $A^+ + B^+$, the kinetic energies released in a given channel are equal for the three molecular species (within the 10% error bar) (Table IV). This result confirms that the multiple-ionization sequence is mainly governed by the Coulombic repulsion of the ion fragments since it involves a coupling which is not molecular specific. However, the dissociative states are certainly not pure Coulombic states since they do not correctly account for the dynamics of the process (cf. Sec. IV A).

V. CONCLUSION

We have investigated the multielectron dissociative ionization of diatomic molecules by intense laser field at a wavelength of 615 nm and, for the first time, a pulse duration of 100 fs. Comparison with previous works clearly shows that the atomic-ion kinetic-energy releases do not depend on the laser-pulse duration (in the range of 100 fs–2 ps) or on the peak laser intensity (in the range of 10^{14} – 5×10^{15} W/cm²). On the contrary, the ionization branching ratios are found to depend strongly on the laser intensity which is the signature of the highly non-linear effects involved in the excitation pattern of the molecule. The fragmentation channels leading to charge-symmetric fragments are widely predominant. Concerning the different molecules investigated in this work, the channel $AB^{2+} \rightarrow A^+ + B^+$ remains molecule specific but the higher charged molecular ions produced during the interaction exhibit the same dissociation energies for N_2 , CO, and O_2 .

The physical interpretation of these results is not straightforward. In particular, a simple model, involving the classical Coulomb repulsion between the atomic-ion fragments, cannot explain the well-defined measured kinetic energies nor the independence of these energies on the laser-pulse rise time. However, this simple picture can constitute a first approach of the excitation pattern of the molecule. Recently a field ionization model was proposed using the Thomas-Fermi-Dirac approximation as a description of the molecule [14]. The predicted branching ratios into different fragmentation channels show a preponderance of charge-symmetric fragmentation and are in good qualitative agreement with the experiments at 600 nm. However, the calculated appearance laser intensities for the different fragmentation channels are definitively larger than those deduced from the experiment. Besides, the dynamics of the molecular excitation, namely, the laser-pulse rise time, is not taken into account in this model. We think that a full quantum treatment where both the electronic and the nuclear motions are quantized is necessary to account for the molecular response. We trust that the extensive experimental data now available will trigger such new theoretical developments.

ACKNOWLEDGMENT

The support of the EEC for the building of the laser system (Grant No. SCI-0103C) is gratefully acknowledged.

- [1] L. J. Frasinski, K. Codling, P. A. Hatherly, J. R. M. Barr, I. N. Ross, and W. T. Toner, *Phys. Rev. Lett.* **58**, 2424 (1987).
- [2] L. J. Frasinski, K. Codling, and P. A. Hatherly, *Phys. Lett. A* **142**, 499 (1989).
- [3] K. Boyer, T. S. Luk, J. C. Solem, and C. K. Rhodes, *Phys. Rev. A* **39**, 1186 (1989).
- [4] C. Cornaggia, J. Lavancier, D. Normand, J. Morellec, and H. X. Liu, *Phys. Rev. A* **42**, 5464 (1990).

- [5] K. Codling, L. J. Frasinski, P. Hatherly, and J. R. M. Barr, *J. Phys. B* **20**, L525 (1987).
- [6] K. Codling, L. J. Frasinski, and P. A. Hatherly, *J. Phys. B* **21**, L433 (1988).
- [7] L. J. Frasinski, K. Codling, and P. A. Hatherly, *Science* **246**, 1029 (1989).
- [8] K. Codling, L. J. Frasinski, P. A. Hatherly, and M. Stankiewicz, *Phys. Scr.* **41**, 433 (1990).
- [9] P. A. Hatherly, L. J. Frasinski, K. Codling, A. J. Langley,

- and W. Shaikh, *J. Phys. B* **23**, L291 (1990).
- [10] J. Lavancier, D. Normand, C. Cornaggia, J. Morellec, and H. X. Liu, *Phys. Rev. A* **43**, 1461 (1991).
- [11] D. Normand, C. Cornaggia, J. Lavancier, J. Morellec, and H. X. Liu, *Phys. Rev. A* **44**, 475 (1991).
- [12] D. Normand, C. Cornaggia, J. Lavancier, and J. Morellec, in *Multiphoton Processes*, Proceedings of the 5th International Conference on Multiphoton Processes, Paris, France, 1990, edited by G. Mainfray and P. Agostini (Commissariat à l'Energie, Gif-sur-Yvette, 1991).
- [13] K. Codling, L. J. Frasinski, and P. A. Hatherly, *J. Phys. B* **22**, L321 (1989).
- [14] M. Brewczyk and L. J. Frasinski, *J. Phys. B* **24**, L307 (1991).
- [15] P. Agostini, P. Breger, A. L'Huillier, H. G. Muller, G. Petite, A. Antonetti, and A. Migus, *Phys. Rev. Lett.* **63**, 2208 (1989), and references therein.
- [16] Z. Bor, *J. Mod. Opt.* **35**, 1907 (1988).
- [17] W. C. Wiley and I. H. McLaren, *Rev. Sci. Instrum.* **26**, 1150 (1955).
- [18] B. L. Schram, A. J. H. Boerboom, W. Kleine, and J. Kistemaker, in *Proceedings of the 7th International Conference on Phenomena in Ionized Gases, Belgrade, 1965*, edited by B. Perovic and D. Tosić (Gradjevinska Knjiga, Belgrade, 1966).
- [19] M. J. Besnard, L. Hellner, G. Dujardin, and D. Winkoun, *J. Chem. Phys.* **88**, 1732 (1988).
- [20] F. Feldmeier, H. Durchholz, and A. Hofmann, *J. Chem. Phys.* **79**, 3789 (1983).
- [21] K. Codling, L. J. Frasinski, and P. A. Hatherly, in *Multiphoton Processes* (Ref. [12]).
- [22] R. R. Freeman, P. H. Bucksbaum, H. Milchberg, S. Darak, D. Schumacher, and M. E. Geusic, *Phys. Rev. Lett.* **59**, 1092 (1987).
- [23] P. Agostini, A. Antonetti, P. Breger, M. Crance, A. Migus, H. G. Muller, and G. Petite, *J. Phys. B* **22**, 1971 (1989).